THE JOURNAL OF PHYSICAL CHEMISTRY C

Article

pubs.acs.org/JPCC

Crystallization-Induced Emission Enhancement of a Simple Tolane-Based Mesogenic Luminogen

Jiaqi Tong,[†] Yi Jia Wang,[†] Zhaoyang Wang,[†] Jing Zhi Sun,[*,†] and Ben Zhong Tang[*,†,‡,§]

[†]MoE Key Laboratory of Macromolecule Synthesis and Functionalization, Department of Polymer Science and Engineering, Zhejiang University, Hangzhou 310027, China

[‡]Guangdong Innovative Research Team, State Key Laboratory of Luminescent Materials and Devices, South China University of Technology, Guangzhou 510640, China

[§]Department of Chemistry, Institute of Molecular Functional Materials, Institute for Advanced Study, The Hong Kong University of Science and Technology, Clear Water Bay, Kowloon, Hong Kong, China

Supporting Information

ABSTRACT: The photophysical properties of a diphenylacetylene derivative (FOEB) were investigated. The fluorescence quantum efficiency (Φ_F, %) of FOEB changes from moderate (49%) to low (9%) and to evidently enhanced (60%) in dilute solution, amorphous solid, and crystal state, respectively. This is a typical phenomenon of crystallization-induced emission enhancement (CIEE). The diphenylacetylene luminogen can be viewed as a propeller-like molecule with two blades (phenyl groups). In solution, the intramolecular rotations of the two blades around the ethynyl unit are activated and partially dissipate the energy in the photoexcited state, thereby leading to emission quenching. Consequently, FOEB exhibits moderate Φ_F in solution. In amorphous solid, the intramolecular rotations are restricted, and a higher Φ_F could be expected. But in fact, the strong $\pi-\pi$ interactions between the luminogens cause heavier emission quenching, and the Φ_F of the molecular aggregates is as low as 9%. In the single crystal, as the crystallographic data revealed, the two phenyl groups in the same diphenylacetylene unit are highly coplanar and the conjugation planes of the two adjacent diphenylacetylene units are orthogonal to each other. Such molecular conformation and chromophore packing eliminate the intermolecular $\pi-\pi$ interaction thereby greatly reducing the $\pi-\pi$ interaction that caused fluorescence quenching, and meanwhile, the orthogonal packing allows the formation of C−H···π bonding between the adjacent phenyl groups to lock the intramolecular rotations and retain fluorescence. As a result, the FOEB single crystal shows evidently enhanced emission. Besides the CIEE property, FOEB demonstrates good liquid crystal property due to the diphenylacetylene mesogen and solvatochromic and mechnochromic effects due to the modification of diphenylacetylene with introduction of electron donor and acceptor functionalities.

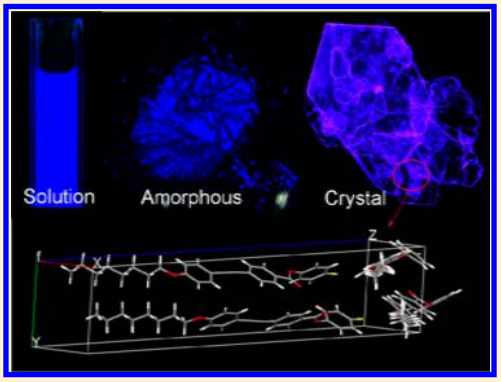

INTRODUCTION

Crystallization-induced emission enhancement (CIEE) refers to a unique photophysical phenomenon in which the compound emits weakly or moderately in amorphous or disordered solids but becomes strongly or very efficiently emissive in crystalline states. the CIEE phenomenon is in contrast to the classical expectation on organic luminogens. As a traditional notion, crystallization and/or orderly packing of the organic luminogens usually leads to luminescent quenching, because the ordered packing allows for the strong intermolecular $\pi-\pi$ interaction, which results in nonradiative decay. To eliminate the intermolecular $\pi-\pi$ interaction, amorphous organic solid with high glass transition temperature (T_g) has been pursued by researchers working in the area of light-emitting materials. But the amorphous state is metastable, and it tends to transform to more stable crystalline phase upon external stimuli such as heating, solvent fuming, and/or electrical field inducing. The CIEE concept has shed new light on the design and synthesis of highly efficient organic/polymeric luminescent materials, which are promising in the application areas of anisotropic light-emitting diodes, optical waveguides, and polarized organic lasers.[1−14] One can make use of the more stable crystalline rather than the metastable amorphous phases of the luminogens to fabricate various devices. Thus, there have been growing interests in developing novel CIEE systems.

Until now, however, organic compounds possessing CIEE characteristic are exiguous because there are no reliable strategies to guide our design and synthesis. It is rational to collect some clues from the accomplished works and the chemical structure of the typical CIEE compounds. The first reported compound with evident CIEE characteristic is 1,1,2,3,4,5-hexaphenylsilole (HPS).[15] The lately reported

Received: June 25, 2015
Revised: September 1, 2015
Published: September 2, 2015

DOI: 10.1021/acs.jpcc.5b06088
J. Phys. Chem. C 2015, 119, 21875−21881

CIEE molecules include 1,2-diphenyl-3,4-bis-(diphenylmethylene)-1-cyclobutene (HPDMCb),[16] diphenyldibenzofulvene (DPDBF) derivatives,[17,18] and tetraphenylethene (TPE) derivatives.[19,20] Summarizing the structural features of these compounds, it can be found that, due to the steric repulsion between the C−H bonds on the adjacent phenyl groups, the whole molecule cannot take a coplanar conformation against the central conjugation unit, but only a propeller shape (see the molecular structures and cartoons in Chart 1). Such kind of twisted conformation prevents strong intermolecular $\pi-\pi$ interaction, and thus helps the photoexcited luminogens decay to the ground state through radiative pathways. Meanwhile, the twisted molecular conformation affords loose molecular packing in the amorphous solid state and the phenyl groups may still rotate or vibrate in some extent; thus the emission of the amorphous solid may be partially exhausted. In a crystal, many weak bonds including C−H···π and C−H···X (X = N, O, F, Cl) interactions help to further rigidify the molecular conformation and block the nonradiative decay. Accordingly, enhanced emission is recorded for the crystallized molecules.

Chart 1. Molecular Structure of CIEE Compounds and the Cartoon of the Propellers

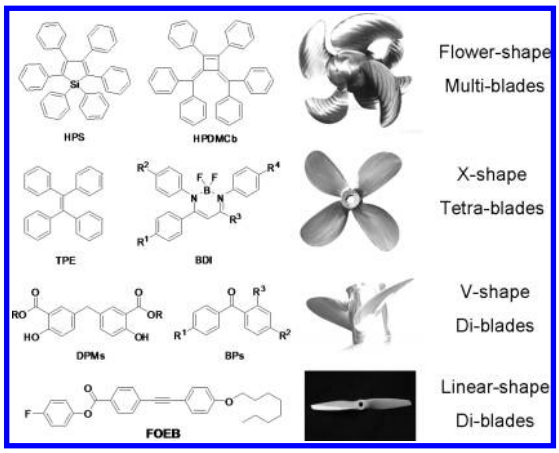

Efficient phosphorescence at room temperature from the crystals of benzophenone derivatives (BPs, Chart 1) were reported in 2010.[21] These molecules have been modified with halogen atoms (F, Cl, Br) at the para positions of the phenyl groups or amino group at the ortho position of benzophenone (Chart 1). All of them are nonemissive whenever they are in dilute solutions, being doped into polymeric matrixes and on the plates of thin layer chromatography. It is believed that the active intramolecular motions including rotations and vibrations effectively annihilate the triplet excitons via nonradiative decay channels. On the contrary, the intramolecular motions in the crystalline state are restricted by the lattices and intermolecular interactions, particularly C−H···O, C−H···X (X = F, Cl, Br), and C−H···π bonding. Thus, the nonradiative decay channels are closed and efficient phosphorescence emits from the crystalline state at room temperature. Lately, CIEE phenomenon was observed for some other compounds containing large electron-negative elements (N, O, F, S), such as carboxyl and phenol decorated diphenylmethane derivatives (DPMs, Chart 1),[22] indigo derivatives,[23] benzimidazole derivatives,[24] borondiiminate (BDI, Chart 1),[25,26] styrylbenzoxazole,[27] *o*-carborane-based anthracene,[28] persulfurated benzene derivative,[29] and diphenyldipyrroethene derivatives.[30] More recently, some complexes (such as BF_2 and gold(I) complexes) have been found to possess CIEE behavior.[31,32]

Looking back to the available CIEE molecules, it is found that all of these molecules share a common structural feature, that is, a propeller-like shape. The benzophenone derivatives (BPs, Chart 1) represent V-shaped luminogens, in which the two phenyl groups can be viewed as two blades on a propeller. A reasonable deduction is that organic luminogens with CIEE characteristic may be derived from other propeller-like conjugated molecules in different configurations such as X-, Y-, and V-shape. On the basis of this assumption, we first pay our attentions to the diphenylacetylene or tolane unit, because it has a linear shape and can be viewed as one of the simplest propellers. Tolane is one of the representative mesogens that are widely used in the construction of liquid crystals (LCs). Its derivatives have shown some advantages including large thresholds, broader nematic phase ranges, and lower melting points.[33−38] Different from other rigid rodlike mesogens such as azobenzene and biphenyl derivative, diphenylacetylene is also a luminogen.[39−42] But the luminescent property of tolane has not attracted much attention although it was incorporated into some fluorescent materials.[43−46] The reason can be mainly ascribed to the efficient crossing of diphenylacetylene's fluorescent singlet to "dark" triplet state.[45,46] Herein, we report the pronounced CIEE property and the mechanistic explanation of a rationally designed diphenylacetylene derivative, together with its solvatochromic behavior, mechanochromic effect, and good LC performance.

RESULTS AND DISCUSSION

Synthesis. The chemical structure of the protocol [4-fluorophenyl 4-((4-(octyloxy)phenyl)ethynyl)-benzoate, FOEB] is shown in Chart 1 (reference Figure 5A and Figure S1 and Scheme S1 in the Supporting Information). Its synthesis and characterization followed the procedures reported in literature.[47,48] The ideas of the molecular design are as follows. On one hand, an electron-donating octyloxy substituent (donor, D) and an electron-accepting ester group (acceptor, A) are attached to the two ends of the central diphenylethynyl core. The D−A effect can lead to higher molecular polarity and a red-shift of emission spectrum. And on the other hand, a fluorine atom is capped on the phenyl ring. It is reported that fluorine modification is helpful to gain large birefringence values and low viscosities, which are important factors for liquid crystal displays with a high response speed.[49,50]

Fluorescent Property. The absorption and emission spectra of FOEB in different solvents are displayed in Figure 1, parts A and B, respectively. In toluene, FOEB shows a sharp absorption band with a maximum at around 325 nm. When the solvent changes from toluene (apolar) to acetonitrile (high polar), the absorption features are nearly identical. On the contrary, the emission features demonstrate evident changes with the changing of the polarity of the solvents. In apolar solvents such as toluene and dioxane, the emission features are characterized by a narrow band with a maximum at 386 nm, which is a typical UV light. In solvents with higher polarity, the emission spectra show evident red-shift. For example, the emission peak of FOEB in acetonitrile solution shifts to 440 nm, which is a pure blue light. Such a bathochromic shift of the emission spectra is a typical solvatochromic phenomenon, and it is ascribed to the D−A structure of FOEB molecule.[51]

DOI: 10.1021/acs.jpcc.5b06088
J. Phys. Chem. C 2015, 119, 21875−21881

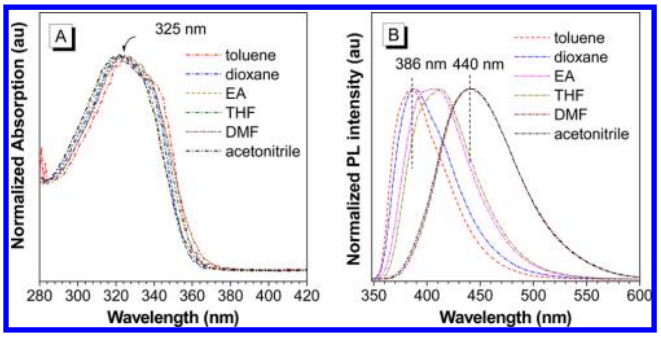

Figure 1. (A) Absorption and (B) photoluminescence (PL) spectra of FOEB in different solvents. The maximal absorption of each solution was used as its excitation wavelength. Concentration of FOEB: 10 μM. Solvents: toluene, 1,4-dioxane, ethyl acetate (EA), THF (tetrahydrofuran), dimethylformamide (DMF), and acetonitrile.

Normally, solvatochromic phenomenon is accompanied by decreasing emission efficiency. We measured the fluorescence quantum efficiency of FOEB in different solvents, and the data are listed in Table S1. The low quantum yield of FOEB in highly polar solvents is attributed to the twisted intramolecular charge-transfer state that acts as a nonradiative decay channel. A quantitative evaluation of the influences of solvent polarity on the bathochromic emission shift is expressed by Lippert–Mataga equation,[52] which describes the relationship between the Stokes shift ($\Delta\nu$, the difference between the maximal wavenumbers of the absorption and emission spectra) and the solvent polarity parameter (Δf) (Figure S2, Supporting Information).

In Aggregation State. The absorption spectra of FOEB in the tetrahydrofuran(THF)/water mixtures with different water fractions (f_w, by volume) are given in Figure 2A. When f_w is

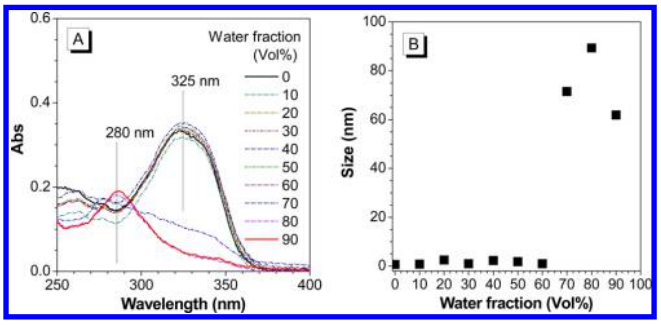

Figure 2. (A) Absorption spectra recorded for FOEB in the mixtures of THF and water with different water fractions (f_w). (B) Plot of the particle sizes of FOEB formed in THF/water at different f_w measured by dynamic light scattering (DLS). Concentration of FOEB: 10 μM.

less than 70%, the absorption spectra show a strong band centered at 325 nm; when f_w increases to or over 70%, the intensity of this absorption band significantly declines and a new band peaked at around 280 nm appears, corresponding to a 45 nm hypsochromic shift. Generally, the hypsochromic shift of the absorption spectrum is associated with the formation of H-aggregate, which is accompanied by an evident emission quenching (cf. Figure 3 and related discussion).[53] To further confirm the aggregate formation, dynamic light scattering (DLS) technique was used to measure the particle sizes in the FOEB solutions with different f_w values, and the data are shown in Figure 2B. As expected, aggregates in testable sizes (with average sizes of 60–90 nm) come into being when the f_w

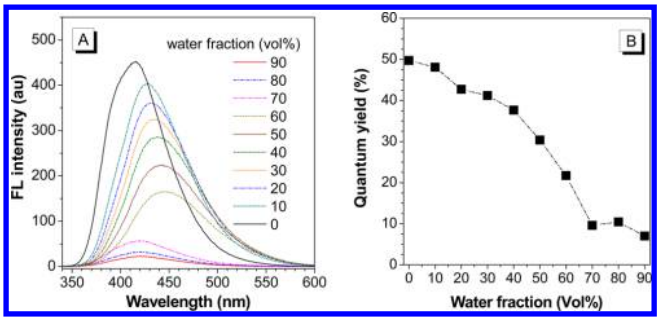

Figure 3. (A) Fluorescence (FL) spectra of FOEB in the mixtures of THF and water with different water fractions f_w. (B) Plots of FL quantum yield (Φ_F) of FOEB vs f_w in THF/water mixtures. The Φ_F values were estimated by using quinine sulfate in 0.1 N H_2SO_4 (Φ_F = 54%) water solution as a standard. Concentration of FOEB = 10 μM.

approaches to or is higher than 70%. Thus, the hypsochromic shift spectral features can be tentatively assigned to the formation of H-aggregate by FOEB molecules.

The changes of the emission features of FOEB in THF/water solutions as a function of f_w have been measured by exciting at 325 nm, and the results are shown in Figure 3A. Meanwhile, the dependence of the emission quantum efficiency (Φ_F) on f_w is given in Figure 3B. The variation trends of the emission features can be largely divided into two regions. In the region where f_w is less than 60%, the fluorescence efficiency shows a monotonous downward trend and the emission peak wavelength shows a gradually bathochromic shift. These observations can be explained by the solvatochromic effect. FOEB is a typical D–A molecule; the intramolecular charge transfer between the D and A moieties is enhanced with the increasing of the environment polarity, which is offered by increasing the water fraction. In the region of f_w > 70%, the solubility of FOEB becomes so low that molecular aggregates generate in the solvent mixture (Figure 2B). The emission intensity displays an evident reduction. By combining the absorption features with the DLS measurement results (reference Figure 1), we assign the aggregation mode of FOEB formed in THF/water mixture with f_w > 70% to H-aggregate. Besides the decrease of emission intensity, when f_w > 70%, the emission peak abruptly blue-shifts from 442 to 418 nm; this can be explained by the solvatochromic effect because the FOEB molecules localize in a less polar environment inside the aggregate.

It is noted that, in Figures 2 and S3, the changes in emission peak wavelength and peak intensity are discrete. Herein the meaning is to reveal that emission species are different in these two regions. When f_w > 70%, the emission comes from the aggregate rather than the isolated FOEB molecules. Furthermore, the quantum yields in solutions with different fractions of water and THF were measured to estimate the fluorescent intensities of FOEB in different states. As can be seen in Figure 3B, the quantum yield presents a downtrend with the increase of f_w, which is in keeping with the appearance of H-aggregates of FOEB.

Thermotropic Liquid Crystalline Property. The thermal stability of FOEB was evaluated by thermogram analysis experiment, and the data indicated that the decomposing temperature of FOEB was about 288 °C at a heating rate of 10 °C/min in N_2 atmosphere (Figure S4, Supporting Information). Meanwhile, we tested the thermal transitions of FOEB, and the representative differential scanning calorimetry (DSC)

DOI: 10.1021/acs.jpcc.5b06088
J. Phys. Chem. C 2015, 119, 21875–21881

traces recorded at a rate of 10 °C/min in the first cooling and the second heating scans are shown in Figure 4. In the heating

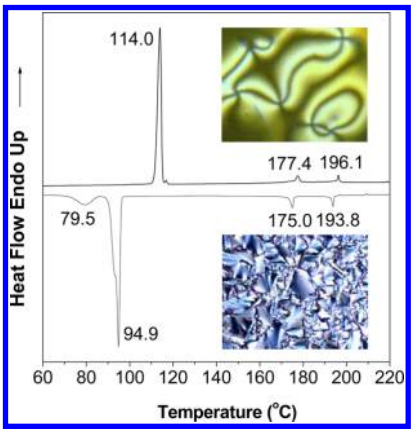

Figure 4. DSC curves of FOEB recorded during the first cooling (upper) and the second heating (lower) processes. Scan rate: 10 °C/min. Inset: polarized optical microscope (POM) images taken on cooling to 195 °C (upper) and 175 °C (lower) from its isotropic state.

run, three phase transitions with sharp endothermic peaks are observed at 114.0, 177.4, and 196.1 °C. To identify their natures, a polarized optical microscope (POM) was used to monitor the phase behaviors. After cooling from the isotropic state to 195 °C, FOEB film displayed a schlieren texture with brush disclination lines (upper image), which is a typical signature for a nematic phase. A focal conic texture was clearly observed after further cooling of FOEB film to 175 °C, which indicated a smectic phase (lower image). Therefore, the sequential transitions at 114.0, 174.1, and 196.1 °C can be assigned to the transitions of crystalline−smectic, smectic−nematic, and nematic−isotropic phase, respectively.

Crystal Structure. To acquire the knowledge of the molecular packing in the LC and solid states and provide structural information relating to the emission properties of FOEB, we grew a single crystal of FOEB by recrystallization from dichloromethane permeated by methanol vapor. The X-ray diffraction analysis results are shown in Figure 5, parts A and B, as well as Tables S2−S7 (CCDC 1018033). The tolane moiety is a rigid rod in the whole, but the two phenyl rings can

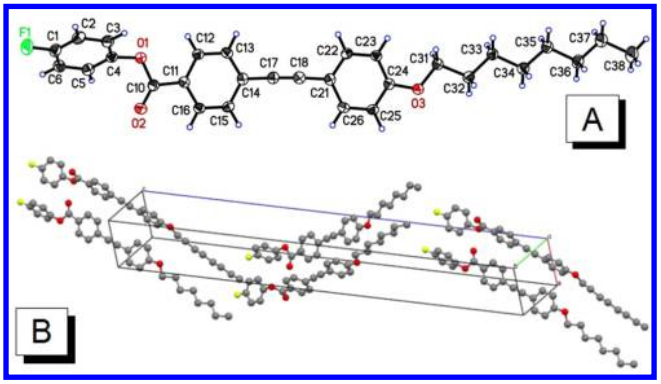

Figure 5. Molecular structure of FOEB (A) and molecular packing in a unit cell (B). The C, O, F, and H atoms are shown in gray, red, green, and blue colors, respectively. All H atoms are omitted in panel B for clarity. The unit cell is assigned to orthorhombic system, and cell dimensions are as follows: a = 5.9834 Å, b = 7.2529 Å, c = 55.184 Å; α = 90°, β = 90°, γ = 90°.

rotate around the central ethyne. This rotational freedom has an impact upon the optical and electronic properties of tolane derivatives. A larger torsional angle between the two phenyls corresponds to a shorter effective conjugation, thereby to a shorter emission wavelength. As revealed by the crystallographic data, the two phenyl rings in the tolane moiety are perfectly coplanar (Table S7, Supporting Information). The planes determined by these two tolane moieties in the adjacent molecules are unparallel. So are the planes of the fluorinated phenol moieties (Figure 5B). Such molecular stacks effectively prevent the intermolecular $\pi-\pi$ interaction, which is propitious to the irradiative decay and the high fluorescent quantum yield in crystalline state.

Crystallization-Induced Emission Enhancement and Mechanochromic Effect. As mentioned above, tolane is not only a mesogen but also a luminogen. The fluorescence spectrum of the FOEB crystal is displayed in Figure 6; the

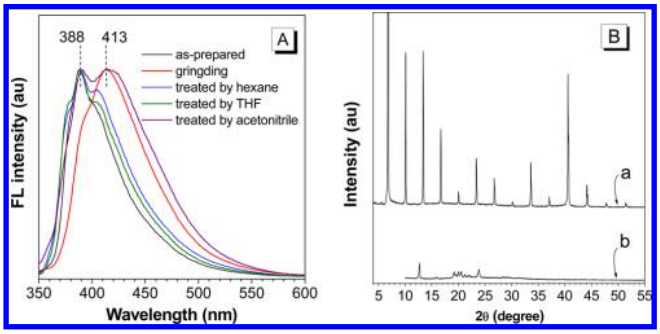

Figure 6. (A) Fluorescence (FL) spectra of FOEB in different states. (B) XRD patterns for FOEB crystal before (curve a) and after (curve b) grinding.

emission maximum locates at around 388 nm. There is only 2 nm of red-shift in comparison with the emission in the toluene solution (see Figure 1B). This result implies very weak electronic interaction between the adjacent FOEB molecules in the crystal, just like the case in dilute solution. The crystallographic data (Figure 6 and Table S2, Supporting Information) provide valuable information about the molecular packing. The two tolane moieties in the adjacent molecules are perpendicular to each other, as determined by the orthogonal crystal system. Consequently, there exists very weak intermolecular $\pi-\pi$ interaction and thereby leads to very limited spectral shift. At the same time, the quantum efficiency (Φ_F) of the FOEB crystal is 60%, as evaluated by using the integrating sphere technique. This value is higher than that measured for FOEB in dilute THF solution (10^{-5} mol/L, Φ_F = 49%). Moreover, in 10^{-6} mol/L hexane solution, the measured Φ_F value is only 18.7%, which is much lower than that of the FOEB crystal and THF solution. This reduction is assigned to the self-absorption of FOEB in hexane solution. As demonstrated by the absorption and emission spectra in Figure S5, an obvious overlap between the absorption and the emission bands is observed. The above data indicate that FOEB is a luminogen possessing the unique property of CIEE.

A red-shifted emission band peak at 413 nm was observed when the crystal sample was ground to a fine powder (Figure 6A). This is a typical mechanochromic phenomenon.[54,55] The emission features of the powder sample largely recovered to the crystalline one when it was treated with several drops of organic solvents such as hexane, THF, or acetonitrile. Annealing the

DOI: 10.1021/acs.jpcc.5b06088
J. Phys. Chem. C 2015, 119, 21875−21881

ground powder with the vapor of these solvents for minutes had the same effect. Sometimes, an emission shoulder with a maximum at around 410 nm could be seen (Figure 6A), due to the fraction that had not recovered to the crystalline state.

To better understand the photophysical properties of FOEB in different states, we measured the Φ_F value of the solids obtained by quenching from nematic and smectic phases with liquid nitrogen, and the data are list in Table S8. The data reveal a trend that the Φ_F is proportional to the order of the solids, since the Φ_F value of the amorphous solid and the solids derived from nematic and smectic phases are 9%, 33%, and 40%, respectively.

Mechanism of CIEE and Mechanochromic Behavior. To understand the origin of the CIEE and mechanochromic behaviors, X-ray diffraction (XRD) measurements were performed on the respective samples, and the diffraction patterns are shown in Figure 6B. Intense and sharp diffraction peaks can be observed for the FOEB crystal. After grinding, the XRD pattern shows significant decreased peak intensity but increased peak widths, suggesting that most of the ordered crystalline material has been eliminated during the grinding process (mechanical force). It is noted that the diffraction peak at the diffraction angle (2θ) of 12.3° is conspicuous in both the XRD patterns of the crystal and ground sample. This peak is assigned to the reflection of the (001) facet, corresponding to the long molecular axis (c axial direction). The vanishing of the diffraction peaks in wide-angle region ($2\theta \sim 30-60°$) of the ground sample implies the ordered long-range molecular packing modes have been destroyed by grinding. The mechanical force induced rearrangement in the a and b axial directions may result in advantageous $\pi-\pi$ interaction between the adjacent tolane moieties. Consequently, the ground powder shows a red-shifted emission feature. We measured the fluorescence quantum yield of the ground sample, and only a result of 9% was recorded, implying the enhanced $\pi-\pi$ interaction.

CONCLUSION

In summary, we have shown that FOEB is a typical lyotropic liquid crystal (LLC) molecule displaying distinct transition points at 114.0, 174.1, and 196.1 °C, which are assigned to the transitions of crystal−smectic, smectic−nematic, and nematic−isotropic phase, respectively. In different solvents, FOEB shows solvatochromic behavior due to the D−A effect of the octyloxyl and 4-fluorophenolester groups. FOEB solid also exhibits moderate mechanochromic effect, which is ascribed to the change in molecular arrangement. In dilute THF solution (10^{-5} mol/L), Φ_F of FOEB is equal to 49%. In crystal and amorphous phases, FOEB emits UV and deep-blue fluorescence with emission maxima at 386 and 413 nm and Φ_F values of 60% and 9%, respectively. The high fluorescence efficiency of the crystal is associated with the orthogonal packing of the tolane moieties in the lattice, which restricts the rotations and of the phenyl groups and simultaneously eliminates the intermolecular $\pi-\pi$ interaction. This is a typical CIEE behavior. In comparison with other reported CIEE molecules, FOEB has a slim shape, small size, and simple structure. It suggests that the tolane unit may be used as a building block to construct more CIEE molecules and achieve better optic/electronic performance in different application areas.

EXPERIMENTAL SECTION

Materials and Instrumentation. The chemical reagents were purchased from commercially available sources and used as received. Tetrahydrofuran was distilled from sodium benzophenone ketyl under nitrogen immediately prior to use. Triethylamine was distilled from KOH under nitrogen. ^{1}H NMR spectra were measured on a Mercury plus 400 MHz NMR spectrometer in $CDCl_3$ using tetramethylsilane (TMS; δ = 0 ppm) as internal standard. Fluorescence spectra were recorded on a spectrofluorophotometer of Shimadzu RF-5301PC. UV−vis absorption spectra were obtained on a Varian Cary 100 Bio UV−vis spectrophotometer. X-ray diffraction measurement was conducted on an XPert Pro instrument. Single-crystal X-ray diffraction intensity data were collected on an Oxford Diffraction Xcalibur Sapphire 3 Gemini Ultra diffractometer; empirical absorption correction was done by using CrysAlis Pro, Oxford Diffraction; the analysis was carried out by using Mercury version 3.3. Polarized optical microscopy was measured on a Nikon E600POL polarizing optical microscope. Thermal behaviors of FOEB were estimated on a PerkinElmer DSC 7 and a PerkinElmer TGA instrument. Relative Φ_F values were estimated by using quinine sulfate in 0.1 N sulfuric acid (Φ_F = 54.6%) as standard. The absorbance of the solution was kept at ∼0.05 to avoid internal filter effect. Absolute Φ_F values were determined by a calibrated integrating sphere with a diameter of 4 in. (Labsphere Inc.).

Synthetic Procedures. The synthesis of the final compound FOEB containing the diphenylacetylene moiety is outlined in Scheme S1. The fluorinated precursor was prepared through esterification of 4-fluorophenol and 4-iodobenzoic acid with *N*,*N*′-dicyclohexyl carbodiimide (DCC) as dehydrating agent, and the other one with the alkyl chain through etherification of 4-iodophenol and 1-bromooctane. By the Sonogashira reaction of terminal alkyne with alkenyl halides catalyzed by Pd(0)/CuI, the target molecule with diphenylacetylene moiety was obtained from the coupling of the precursors with alkyne. The detailed procedures are described in the Supporting Information, and the spectral data of structural characterization are also included in the Supporting Information. The thermal properties of FOEB were investigated by using thermogravimetric analysis (TGA); FOEB possesses high thermal stability with a decomposition temperature (T_d) at 328 °C.

ASSOCIATED CONTENT

Supporting Information

The Supporting Information is available free of charge on the ACS Publications website at DOI: 10.1021/acs.jpcc.5b06088.

The synthetic scheme (Scheme S1), ^{1}H NMR spectrum, thermogravimetric analysis (TGA), solvatochromism calculation and the plot of Stokes shift ($\Delta\nu$) of FOEB in each solvent vs Δf of the respective solvent, and crystal data and structure refinement for FOEB (Tables S1−S6) (PDF)

AUTHOR INFORMATION

Corresponding Authors

*Phone: +86-571-87953734. Fax: +86-571-87953734. E-mail: sunjz@zju.edu.cn.

*Phone: +852-2358-7375. Fax: +852-2358-1594. E-mail: tangbenz@ust.hk.

DOI: 10.1021/acs.jpcc.5b06088
J. Phys. Chem. C 2015, 119, 21875−21881

Notes

The authors declare no competing financial interest.

■ ACKNOWLEDGMENTS

This work was supported partly by the National Basic Research Program of China (2013CB834704), the National Science Foundation of China (51273175). B.Z.T. thanks the support of the Guangdong Innovative Research Team Program of China (20110C0105067115), the Research Grants Council of Hong Kong (16301614, N_HKUST604/14 and N_HKUST620/11), the Innovation and Technology Commission (ITCPD/17-9), and the University Grants Committee of Hong Kong (AoE/P-03/08 and T23-713/11-1). J.Z.S. thanks the support from Jiangsu Key Laboratory of Advanced Functional Polymer Design and Application (Soochow University).

■ REFERENCES

(1) Yashima, S.; Tanabe, K.; Sagara, Y. *Stimuli-Responsive Photoluminescent Liquid Crystals*; Springer-Verlag: Berlin, Germany, 2012.

(2) Wong, K. M.-C.; Yam, V. W.-W. Self-Assembly of Luminescent Alkynylplatinum(II) Terpyridyl Complexes: Modulation of Photophysical Properties through Aggregation Behavior. *Acc. Chem. Res.* **2011**, *44*, 424−434.

(3) Romero-Nieto, C.; Marcos, M.; Merino, S.; Barberá, J.; Baumgartner, T.; Rodríguez-López, J. Room Temperature Multifunctional Organophosphorus Gels and Liquid Crystals. *Adv. Funct. Mater.* **2011**, *21*, 4088−4099.

(4) Girotto, E.; Eccher, J.; Vieira, A. A.; Bechtold, I. H.; Gallardo, H. Luminescent Columnar Liquid Crystals Based on 1,3,4-Oxadiazole. *Tetrahedron* **2014**, *70*, 3355−3360.

(5) Beltran, E.; Robles-Hernández, B.; Sebastian, N.; Serrano, J. L.; Giménez, R.; Sierra, T. Bent-core Luminescent and Electroactive Bis(triazolyl)triazines with Compact Columnar Mesomorphism. *RSC Adv.* **2014**, *4*, 23554−23561.

(6) Eccher, J.; Faria, G. C.; Bock, H.; von Seggern, H.; Bechtold, I. H. Order Induced Charge Carrier Mobility Enhancement in Columnar Liquid Crystal Diodes. *ACS Appl. Mater. Interfaces* **2013**, *5*, 11935−11943.

(7) Dambal, H. K.; Yelamaggad, C. V. Technologically Promising, Room Temperature Luminescent Columnar Liquid Crystals Derived from *s*-Triazine Core: Molecular Design, Synthesis and Characterization. *Tetrahedron Lett.* **2012**, *53*, 186−190.

(8) Sagara, Y.; Komatsu, T.; Ueno, T.; Hanaoka, K.; Kato, T.; Nagano, T. Covalent Attachment of Mechanoresponsive Luminescent Micelles to Glasses and Polymers in Aqueous Conditions. *J. Am. Chem. Soc.* **2014**, *136*, 4273−4280.

(9) Zabulica, A.; Perju, E.; Bruma, M.; Marin, L. Novel Luminescent Liquid Crystalline Polyazomethines. Synthesis and Study of Thermotropic and Photoluminescent Properties. *Liq. Cryst.* **2014**, *41*, 252−262.

(10) Yamane, S.; Sagara, Y.; Mutai, T.; Araki, K.; Kato, T. Mechanochromic Luminescent Liquid Crystals Based on a Bianthryl Moiety. *J. Mater. Chem. C* **2013**, *1*, 2648−2656.

(11) Marin, L.; Zabulica, A.; Sava, M. Symmetric Liquid Crystal Dimers Containing a Luminescent Mesogen: Synthesis, Mesomorphic Behavior, and Optical Properties. *Soft Mater.* **2013**, *11*, 32−39.

(12) Senyuk, B.; Behabtu, N.; Pacheco, B. G.; Lee, T.; Ceriotti, G.; Tour, J. M.; Pasquali, M.; Smalyukh, I. I. Nonlinear Photoluminescence Imaging of Isotropic and Liquid Crystalline Dispersions of Graphene Oxide. *ACS Nano* **2012**, *6*, 8060−8066.

(13) Han, T.; Feng, X.; Chen, D.; Dong, Y. A Diethylaminophenol Functionalized Schiff Base: Crystallization-Induced Emission-Enhancement, Switchable Fluorescence and Application for Security Printing and Data Storage. *J. Mater. Chem. C* **2015**, *3*, 7446−7454.

(14) Lin, Y.; Chen, G.; Zhao, L.; Yuan, W. Z.; Zhang, Y.; Tang, B. Z. Diethylamino Functionalized Tetraphenylethenes: Structural and Electronic Modulation of Photophysical Properties, Implication for the CIE Mechanism and Application to Cell Imaging. *J. Mater. Chem. C* **2015**, *3*, 112−120.

(15) Dong, Y.; Lam, J. W. Y.; Qin, A.; Li, Z.; Sun, J.; Dong, Y.; Tang, B. Z. Vapochromism and Crystallization-Enhanced Emission of 1,1-Disubstituted 2,3,4,5-Tetraphenylsiloles. *J. Inorg. Organomet. Polym. Mater.* **2007**, *17*, 673−678.

(16) Dong, Y. Q.; Lam, J. W. Y.; Qin, A.; Sun, J. X.; Liu, J. Z.; Li, Z.; Sun, J. Z.; Sung, H. H. Y.; Williams, I. D.; Kwok, H. S.; Tang, B. Z.; et al. Aggregation-Induced and Crystallization-Enhanced Emission of 1,2-Diphenyl-3,4-bis(diphenylmethylene)-1-cyclobutene. *Chem. Commun.* **2007**, *31*, 3255−3257.

(17) Dong, Y.; Lam, J. W. Y.; Qin, A.; Li, Z.; Sun, J. Z.; Sung, H. H. Y.; Williams, I. D.; Tang, B. Z. Switching the Light Emission of (4-Biphenyl)phenyldibenzofulvene by Morphological Modulation: Crystallization-Induced Emission Enhancement. *Chem. Commun.* **2007**, *1*, 40−42.

(18) Luo, X. L.; Li, J. N.; Li, C. H.; Heng, L. P.; Dong, Y. Q.; Liu, Z. P.; Bo, Z. S.; Tang, B. Z. Reversible Switching of the Emission of Diphenyldibenzofulvenes by Thermal and Mechanical Stimuli. *Adv. Mater.* **2011**, *23*, 3261−3265.

(19) Zhao, N.; Yang, Z.; Lam, J. W. Y.; Sung, H. H. Y.; Xie, N.; Chen, S.; Su, H.; Gao, M.; Williams, I. D.; Wong, K. S.; et al. Benzothiazolium-Functionalized tetraphenylethene: an AIE Luminogen with Tunable Solid-State Emission. *Chem. Commun.* **2012**, *48*, 8637−8639.

(20) Yuan, W. Z.; Gong, Y.; Chen, S.; Shen, X. Y.; Lam, J. W. Y.; Lu, P.; Lu, Y.; Wang, Z.; Hu, R.; Xie, N.; et al. Efficient Solid Emitters with Aggregation-Induced Emission and Intramolecular Charge Transfer Characteristics: Molecular Design, Synthesis, Photophysical Behaviors, and OLED Application. *Chem. Mater.* **2012**, *24*, 1518−1528.

(21) Yuan, W. Z.; Shen, X. Y.; Zhao, H.; Lam, J. W. Y.; Tang, L.; Lu, P.; Wang, C.; Liu, Y.; Wang, Z.; Zheng, Q.; et al. Crystallization-Induced Phosphorescence of Pure Organic Luminogens at Room Temperature. *J. Phys. Chem. C* **2010**, *114*, 6090−6099.

(22) Guieu, S.; Rocha, J.; Silva, A. M. S. Crystallization-Induced Light-Emission Enhancement of Diphenylmethane Derivatives. *Tetrahedron* **2013**, *69*, 9329−9334.

(23) Yang, C.; Trinh, Q. T.; Wang, X.; Tang, Y.; Wang, K.; Huang, S.; Chen, X.; Mushrif, S. H.; Wang, M. Crystallization-Induced Red Emission of a Facilely Synthesized Biodegradable Indigo Derivative. *Chem. Commun.* **2015**, *51*, 3375−3378.

(24) Cao, Y.; Yang, M.; Wang, Y.; Zhou, H. P.; Zheng, J.; Zhang, X.; Wu, J.; Tian, Y.; Wu, Z. Aggregation-Induced and Crystallization-Enhanced Emissions with Time-Dependence of a New Schiff-Base Family Based on Benzimidazole. *J. Mater. Chem. C* **2014**, *2*, 3686−3694.

(25) Yoshii, R.; Hirose, A.; Tanaka, K.; Chujo, Y. Functionalization of Boron Diiminates with Unique Optical Properties: Multicolor Tuning of Crystallization-Induced Emission and Introduction into the Main Chain of Conjugated Polymers. *J. Am. Chem. Soc.* **2014**, *136*, 18131−18139.

(26) Yoshii, R.; Hirose, A.; Tanaka, K.; Chujo, Y. Boron Diiminate with Aggregation-Induced Emission and Crystallization-Induced Emission-Enhancement Characteristics. *Chem.—Eur. J.* **2014**, *20*, 8320−8324.

(27) Xue, P.; Yao, B.; Sun, J.; Zhang, Z.; Li, K.; Liu, B.; Lu, R. Crystallization-Induced Emission of Styrylbenzoxazole Derivate with Response to Proton. *Dyes Pigm.* **2015**, *112*, 255−261.

(28) Naito, H.; Morisaki, Y.; Chujo, Y. *o*-Carborane-Based Anthracene: A Variety of Emission Behaviors. *Angew. Chem., Int. Ed.* **2015**, *54*, 5084−5087.

(29) Fermi, A.; Bergamini, G.; Peresutti, R.; Marchi, E.; Roy, M.; Ceroni, P.; Gingras, M. Molecular Asterisks with a Persulfurated Benzene Core are among the Strongest Organic Phosphorescent Emitters in the Solid State. *Dyes Pigm.* **2014**, *110*, 113−122.

(30) Garg, K.; Ganapathi, E.; Rajakannu, P.; Ravikanth, M. Stereochemical Modulation of Emission Behaviour in *E*/*Z* Isomers of Diphenyldipyrroethene from Aggregation Induced Emission to

DOI: 10.1021/acs.jpcc.5b06088
J. Phys. Chem. C 2015, 119, 21875−21881

Crystallization Induced Emission. *Phys. Chem. Chem. Phys.* **2015**, *17*, 19465−19473.
(31) Galer, P.; Korošec, R. C.; Vidmar, M.; Šket, B. Crystal Structures and Emission Properties of the BF_2 Complex 1-Phenyl-3-(3,5-dimethoxyphenyl)-propane-1,3-dione: Multiple Chromisms, Aggregation- or Crystallization-Induced Emission, and the Self-Assembly Effect. *J. Am. Chem. Soc.* **2014**, *136*, 7383−7394.
(32) Chen, Z.; Zhang, J.; Song, M.; Yin, J.; Yu, G.-A.; Liu, S. H. A Novel Fluorene-Based Aggregation-Induced Emission (AIE)-Active Gold(I) Complex with Crystallization-Induced Emission Enhancement (CIEE) and Reversible Mechanochromism Characteristics. *Chem. Commun.* **2015**, *51*, 326−329.
(33) Chen, H.; Liu, P.; Li, H.; Daniel, S.; Zeng, Z. 3,4-Difluoropyrrole-, 3,3,4,4-Tetrafluoropyrrolidine-Based Tolan Liquid Crystals. *Tetrahedron* **2013**, *69*, 5129−5135.
(34) Chen, X.; Shen, Y.; Wen, J. Synthesis and Mesomorphic Properties of Tolane-Based Fluorinated Liquid Crystals with an Acrylate Linkage. *Mol. Cryst. Liq. Cryst.* **2010**, *528*, 138−146.
(35) Arakawa, Y.; Kang, S.; Nakajima, S.; Sakajiri, K.; Cho, Y.; Kawauchi, S.; Watanabe, J.; Konishi, G. Diphenyltriacetylenes: Novel Nematic Liquid Crystal Materials and Analysis of their Nematic Phase-Transition and Birefringence Behaviours. *J. Mater. Chem. C* **2013**, *1*, 8094−8102.
(36) Khoo, I. C.; Webster, S.; Kubo, S.; Youngblood, W. J.; Liou, J. D.; Mallouk, T. E.; Lin, P.; Hagan, D. J.; Van Stryland, E. W. Synthesis and Characterization of the Multi-Photon Absorption and Excited-State Properties of a Neat Liquid 4-Propyl 4′-butyl Diphenyl Acetylene. *J. Mater. Chem.* **2009**, *19*, 7525−7531.
(37) Marwitz, A. J. V.; Lamm, A. N.; Zakharov, L. N.; Vasiliu, M.; Dixon, D. A.; Liu, S.-Y. BN-Substituted Diphenylacetylene: a Basic Model for Conjugated π-Systems Containing the BN Bond Pair. *Chem. Sci.* **2012**, *3*, 825−829.
(38) Lingard, H.; Han, J. T.; Thompson, A. L.; Leung, I. K. H.; Scott, R. T. W.; Thompson, S.; Hamilton, A. D. Diphenylacetylene-Linked Peptide Strands Induce Bidirectional β-Sheet Formation. *Angew. Chem., Int. Ed.* **2014**, *53*, 3650−3653.
(39) Yelamaggad, C. V.; Shashikala, I. S.; Hiremath, U. S.; Shankar Rao, D. S.; Prasad, S. K. Liquid Crystal Dimers Possessing Chiral Rod-Like Anisometric Segments: Synthesis, Characterization and Electro-Optic Behaviour. *Liq. Cryst.* **2007**, *34*, 153−167.
(40) Hird, M. Fluorinated Liquid Crystals-Properties and Applications. *Chem. Soc. Rev.* **2007**, *36*, 2070−2095.
(41) Yuan, W. Z.; Yu, Z.-Q.; Lu, P.; Deng, C.; Lam, J. W. Y.; Wang, Z.; Chen, E.-Q.; Ma, Y.; Tang, B. Z. High Efficiency Luminescent Liquid Crystal: Aggregation-Induced Emission Strategy and Biaxially Oriented Mesomorphic Structure. *J. Mater. Chem.* **2012**, *22*, 3323−3326.
(42) Chen, Y. F.; Lin, J. S.; Yuan, W. Z.; Yu, Z. Q.; Lam, J. W. Y.; Tang, B. Z. 1-((12-Bromododecyl)oxy)-4-((4-(4-pentylcyclohexyl)-phenyl)ethynyl)benzene: Liquid Crystal with Aggregation-Induced Emission Characteristics. *Sci. China: Chem.* **2013**, *56*, 1191−1196.
(43) Taylor, T. J.; Elbjeirami, O.; Burress, C. N.; Tsunoda, M.; Bodine, M. I.; Omary, M. A.; Gabbai, F. P. Complexation of Tolane by Fluorinated Organomercurials − Structures and Luminescence Properties of an Unusual Class of Supramolecular π-Coordination Polymers. *J. Inorg. Organomet. Polym. Mater.* **2008**, *18*, 175−179.
(44) Zhao, D.; Xu, Z.; Wang, G.; Cao, H.; Li, W.; He, W.; Huang, W.; Yang, Z.; Yang, H. Formation of Surface Relief Gratings with Homeotropically Oriented Photopolymer from a Photocross-Linkable Organic Monomer. *Phys. Chem. Chem. Phys.* **2010**, *12*, 1436−1439.
(45) Saltiel, J.; Kumar, V. K. R. Photophysics of Diphenylacetylene: Light from the "Dark State. *J. Phys. Chem. A* **2012**, *116*, 10548−10558.
(46) Zgierski, M. Z.; Lim, E. C. Nature of the 'Dark' State in Diphenylacetylene and Related Molecules: State Switch from the Linear π-π^* State to the Bent π-σ^* State. *Chem. Phys. Lett.* **2004**, *387*, 352−355.
(47) Yang, Y.-G.; Chen, H.; Tang, G.; Wen, J.-X. Synthesis and Mesomorphic Properties of Several Series of Fluorinated Ester Liquid Crystals. *Liq. Cryst.* **2002**, *29*, 255−261.
(48) Yang, Y.-G.; Wang, K.; Wen, J. X. Synthesis and Mesomorphic Properties of some Fluorinated Phenyl 4-[(4-*n*-alkoxyphenyl)ethynyl]-benzoates. *Liq. Cryst.* **2001**, *28*, 1553−1559.
(49) Simpson, S. H.; Richardson, R. M.; Hanna, S. Influence of Dye Molecules on the Birefringence of Liquid Crystal Mixtures at Near Infrared Frequencies. *J. Chem. Phys.* **2007**, *127*, 104901−104914.
(50) Yang, Y.; Li, H.; Wen, J. Synthesis and Mesomorphic Properties of Chiral Fluorinated Liquid Crystals. *Liq. Cryst.* **2007**, *34*, 975−979.
(51) Reichardt, C. Solvatochromic Dyes as Solvent Polarity Indicators. *Chem. Rev.* **1994**, *94*, 2319−2358.
(52) Li, J.; Zhao, N.; Li, Y.; Li, B.; Yang, Y. Mesomorphism Behavior of Two Series of Chiral Compounds with Semiperfluorocarbon Chains. *Mol. Cryst. Liq. Cryst.* **2012**, *562*, 123−132.
(53) Spano, F. C. The Spectral Signatures of Frenkel Polarons in H- and J-Aggreates. *Acc. Chem. Res.* **2010**, *43*, 429−439.
(54) Zhang, X.; Chi, Z.; Zhang, Y.; Liu, S.; Xu, J. Recent Advances in Mechanochromic Luminescent Metal Complexes. *J. Mater. Chem. C* **2013**, *1*, 3376−3390.
(55) Mei, J.; Hong, Y.; Lam, J. W. Y.; Qin, A.; Tang, Y.; Tang, B. Z. Aggregation-Induced Emission: The Whole Is More Brilliant than the Parts. *Adv. Mater.* **2014**, *26*, 5429−5479.

DOI: 10.1021/acs.jpcc.5b06088
J. Phys. Chem. C 2015, 119, 21875−21881